Accepted Manuscript

Aryl thiosemicarbazones for the treatment of trypanosomatidic infections

Pasquale Linciano, Carolina B. Moraes, Laura M. Alcantara, Caio H. Franco, Bruno Pascoalino, Lucio H. Freitas-Junior, Sara Macedo, Nuno Santarem, Anabela Cordeiro-da-Silva, Sheraz Gul, Gesa Witt, Maria Kuzikov, Bernhard Ellinger, Stefania Ferrari, Rosaria Luciani, Antonio Quotadamo, Luca Costantino, Maria Paola Costi

PII: S0223-5234(18)30056-4

DOI: 10.1016/j.ejmech.2018.01.043

Reference: EJMECH 10120

To appear in: *European Journal of Medicinal Chemistry*

Received Date: 15 August 2017

Revised Date: 12 January 2018

Accepted Date: 14 January 2018

Please cite this article as: P. Linciano, C.B. Moraes, L.M. Alcantara, C.H. Franco, B. Pascoalino, L.H. Freitas-Junior, S. Macedo, N. Santarem, A. Cordeiro-da-Silva, S. Gul, G. Witt, M. Kuzikov, B. Ellinger, S. Ferrari, R. Luciani, A. Quotadamo, L. Costantino, M.P. Costi, Aryl thiosemicarbazones for the treatment of trypanosomatidic infections, *European Journal of Medicinal Chemistry* (2018), doi: 10.1016/j.ejmech.2018.01.043.

Aryl thiosemicarbazones for the treatment of trypanosomatidic infections

Pasquale Linciano[a], Carolina B. Moraes[b], Laura M. Alcantara[b], Caio H. Franco[b], Bruno Pascoalino[b], Lucio H. Freitas-Junior[b], Sara Macedo[c], Nuno Santarem[c], Anabela Cordeiro-da-Silva[c,d], Sheraz Gul[e], Gesa Witt[e], Maria Kuzikov[e], Bernhard Ellinger[e], Stefania Ferrari[a], Rosaria Luciani[a], Antonio Quotadamo[a], Luca Costantino[a], Maria Paola Costi[a*]

[a]University of Modena and Reggio Emilia, Via Campi 103, 41125 Modena, Italy; [b]Brazilian Biosciences National Laboratory (LNBio), Brazilian Center for Research in Energy and Materials (CNPEM), 13083-970, Campinas - SP, Brazil; [c]Institute for Molecular and Cell Biology, 4150-180 Porto, Portugal" with "Instituto de Investigação e Inovação em Saúde, Universidade do Porto and Institute for Molecular and Cell Biology, 4150-180 Porto, Portugal; [d]Departamento de Ciências Biológicas, Faculdade de Farmácia, Universidade do Porto, Porto, Portugal. [e]Fraunhofer Institute for Molecular Biology and Applied Ecology Screening Port, Hamburg, Germany.

ABSTRACT: Basing on a library of thiadiazole derivatives showing anti-trypanosomatidic activity, we have considered the thiadiazoles opened forms and reaction intermediates, thiosemicarbazones, as compounds of interest for phenotypic screening against *Trypanosoma brucei (Tb),* intracellular amastigote form of *Leishmania infantum (Li)* and *Trypanosoma cruzi (Tc)*. Similar compounds have already shown interesting activity against the same organisms. The compounds were particularly effective against *T.brucei* and *T.cruzi*. Among the 28 synthesized compounds, the best one was (E)-2-(4-((3.4-dichlorobenzyl)oxy)benzylidene) hydrazinecarbothioamide (**A14**) yielding a comparable anti-parasitic activity against the three parasitic species (*Tb*EC_{50} = 2.31 μM, *Li*EC_{50} = 6.14 μM, *Tc*EC_{50} = 1.31 μM) and a Selectivity Index higher than 10 with respect to human macrophages, therefore showing a pan-anti-trypanosomatidic activity. (E)-2-((3'.4'-dimethoxy-[1.1'-biphenyl]-3-yl)methyle ne) hydrazinecarbothioamide (**A12*)*** and (E)-2-(4-((3.4-dichlorobenzyl)oxy)benzylidene)hydrazine carbothioamide (**A14**) were able to potentiate the anti-parasitic activity of methotrexate (MTX) when evaluated in combination against *T. brucei*, yielding a 6-fold and 4-fold respectively Dose Reduction Index for MTX. The toxicity profile against four human cell lines and a panel of *in vitro* early-toxicity assays (comprising *h*ERG, Aurora B, five cytochrome P450 isoforms and mitochondrial toxicity) demonstrated the low toxicity for the thosemicarbazones class in comparison with known drugs. The results confirmed thiosemicarbazones as a suitable chemical scaffold with potential for the development of properly decorated new anti-parasitic drugs.

Keywords. Thiosemicarbazone, *Trypanosoma brucei*, *Trypanosoma cruzi*, *Leishmania infantum*, Early-toxicity, pan-anti-trypanosomatidic activity.

1. Introduction

Trypanosomatids of the genera *Trypanosoma* and *Leishmania* are infectious agents of three important neglected tropical diseases such as human African trypanosomiasis (HAT) [1,2], Chagas disease [3] and visceral and cutaneous leishmaniasis. [4]. The treatment of these parasitic infections relies on pentamidine (PEN) (Figure 1), suramine and melarsoprol as the first choice drugs for the treatment of HAT [5], whereas benznidazole (BZD) (Figure 1) and nifurtimox are routinely used for the treatment of Chagas disease. [6,7] The current therapy of leishmaniasis is based on antimonial organic complexes (*i.e.* sodium stibogluconate and meglumine antimoniate) and amphotericin B (AmB). [4] In 2002, the Indian government approved miltefosine (MIL) as the first oral antileishmanial agent (Figure 1). [8]

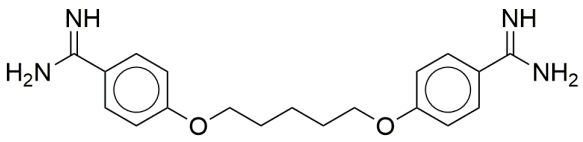

Pentamidine

T. brucei EC_{50} = 3.80 nM

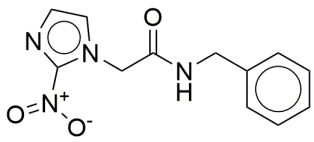

Benznidazole

Amastigote form of *T. cruzi* EC_{50} = 2.40 μM

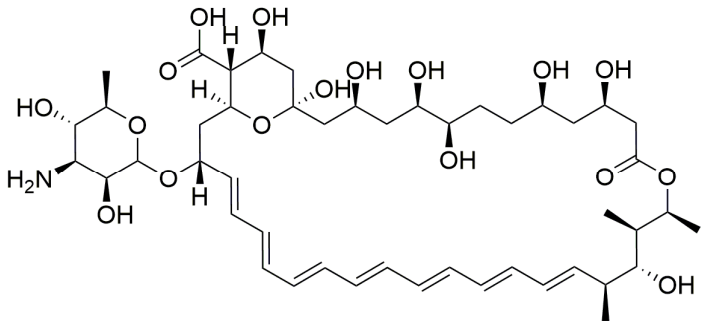

Amphotericin B

Amastigote form of *L. infantum* EC_{50} = 1.14 μM

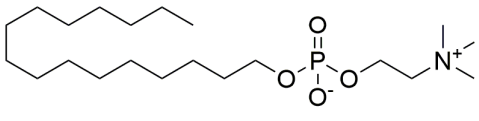

Miltefosine

Amastigote form of *L. infantum* EC_{50} = 1.29 μM

Figure 1. Chemical structures of first choice drugs used for the treatment of HAT, Chagas disease and leishmaniasis, respectively, assumed as reference compounds in our system.

All these old drugs suffer from high toxicity and development of resistance. [9] Thus, the discovery of new chemotherapeutic agents is urgently required. [2] A phenotypic screening approach has been

recently very successful in the discovery of new drug candidates within this therapeutic area, this being illustrated by fexinidazole and the oxaborole SCYX-7158 recently progressed into clinical trials for the treatment of HAT. [10] Fexinidazole and another nitroimidazole (DNDI-VL-2098) are under preclinical evaluation as anti-leishmanial oral drugs in animal models of the diseases. [11,12]

We have previously identified different compound classes with interesting activity profile against *T. brucei*, the intracellular amastigote stage of *L. infantum* and of *T. cruzi*. [13] Among them flavonoids [14], chalcones [15] and thiadiazoles [16] showed anti-parasitic activity with EC_{50} in the micromolar range. The anti-parasitic activity was sometimes associated with the capability to inhibit enzymes of the folate pathway such as pteridine reductase 1 (PTR1) and dihydrofolate reductase (DHFR) [14-17]. Combinations with the known antifolate methotrexate (MTX) were also studied based on the principle of inactivation of the folate pathway in trypanosomatids through combined inhibition of PTR1 and DHFR. [14,16] Synergic effects were observed for the compounds that showed PTR1 inhibition (*i.e.* thiadiazoles) [16] but also with compounds that did not show anti-folate enzymes activity (*i.e.* flavonoids) [14], suggesting that the successful synergic combination may also involve multi-targeting inhibitors. The biochemical mechanism for the latter synergic combination effect is under study. In particular one of the best compounds discovered was (3-hydroxy-6-methoxy-2-(4- methoxyphenyl)-4H-chromen-4-one), a flavonoid derivative that showed a synergic effect in combination with MTX with EC_{50} potentiation around 8-folds and was considered a promising candidate for pharmacokinetic studies [14].

In our effort to develop further the thiadiazole derivatives against *T. brucei*, we identified the thiosemicarbazones. From a chemical point of view, thiosemicarbazones are intermediates for the synthesis of 2-amino-1,3,4-thiadiazoles and they exist in solution at equilibrium between the open-chain and ring-closed form (ring-chain tautomerism) (Figure 2) [18][19], where the open form is synthetically easily accessible. The thiosemicarbazone scaffold was already known in the field of anti-parasitic agents. Thiosemicarbazones were originally designed as parasitic cysteine protease inhibitors such us cruzain, in *T. cruzi*, and rodhesain in *T. brucei*, two enzymes which play a vital

role at every stage of the parasite's life cycle. Several members of this class of compounds, inactive on the enzyme, were active on parasites, suggesting that cruzain was only one of the targets for some of these compounds. [20–25] The formation of strong metal chelating thiosemicarbazones or their metal-complexes [26–29] suggested that the mechanism of action is mainly due to a dual pathway involving production of toxic free radicals by thiosemicarbazone bioreduction or metal complex-DNA interaction.[30]

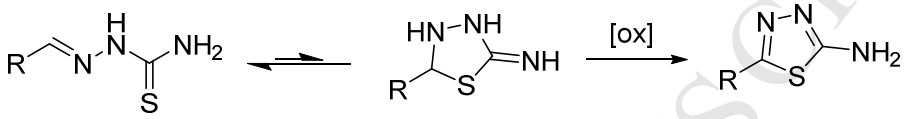

Figure 2. Ring-chain tautomerism of thiosemicarbazone and oxidation of the cyclic form to 2-amino-1,3,4-thiadiazole.

In the present work, we opted for enlarging the thiosemicarbazone scaffold to explore further the anti-parasitic activity through phenotypic screening. We evaluated first the 14 thiosemicarbazones related to the 2-amino-1,3,4-thiadiazoles presented in our previous work, and then, in a ligand based design approach, we prepared 14 new thiosemicarbazones exploring the effect of diverse substituents on the anti-parasitic activity. All compounds were evaluated in phenotypic screening assays against *T. brucei* and the intracellular amastigote stage of *L. infantum* and *T. cruzi*. The most promising compounds were subsequently evaluated in a panel of *in vitro* early toxicity assays which comprised *h*ERG, Aurora B, five cytochrome P450 isoforms (1A2, 2C9, 2C19, 2D6, 3A4) and mitochondrial toxicity (786-O cell-line), cytotoxicity (A549 and WI-38 cell-lines) and selectivity against two human cell lines (THP-1 macrophages and U2OS osteosarcoma cells). Combination studies were also performed with methotrexate (MTX) for all the active compounds against *T. brucei*.

2. Results and Discussion

2.1. Thiosemicarbazones design and synthesis

The first library of thiosemicarbazones **A1-14** (Table 1) were intermediates for the synthesis of the related thiadiazoles **B1-14** previously studied (Table SI-1)**.** [31] Subsequently, with the purpose to explore a primary structure-activity relationship and to identify the molecular features that are favorable and those that are detrimental to the activity a second library of fourteen new analogous (**A15-28**) were prepared. The thiosemicarbazone moiety was retained unaltered. A wider range of substituents of the aromatic portion possessing diverse steric and electronic behavior were explored for their capability to modulate antiparasitic activities and other properties of the future drug molecule such as selectivity, satisfactory ADME and early toxicity profiles (Table 1).

Table 1. Chemical structures and anti-parasitic activities against *T. brucei*, and the amastigote form of *L. infantum* and *T. cruzi* of thiosemicarbazones **A1-A28.**

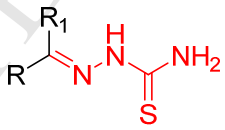

Compound	Chemical Structure		Anti-parasitic % cell growth inhibition at 50 µM [EC_{50} in µM][a,b]		
	R	R_1	*T.brucei*	*L. infantum*	*T. cruzi*
A1	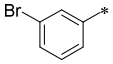	-H	44.08	NI	90.77 [2.29]
A2		-H	87.26 [31.50]	NI	91.46 [15]
A3	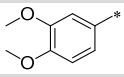	-H	30.57	NI	36.94
A4	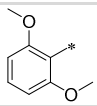	-H	NI	25.29	74.26
A5	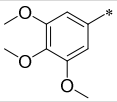	-H	0.21	7.19	NI

A6	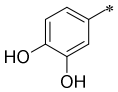	-H	109.4 [27.13]	9.41	59.97
A7	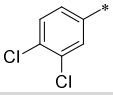	-H	NI	17.59	23.13
A8		-H	NI	26.85	93.58 [1.87]
A9	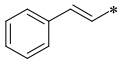	-H	91.7 [16.88]	45.88	94.59 [1.59]
A10	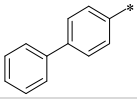	-H	NI	NI	95.18 [4.17]
A11	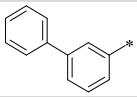	-H	0.9	35.75	20.23
A12	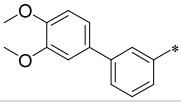	-H	93.86 [7.45]	NI	82.41 [29.5]
A13	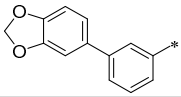	-H	61.75	46.91	71.26
A14	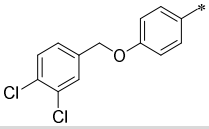	-H	100.2 [2.31]	80.53 [6.14]	80.49 [1.31]
A15	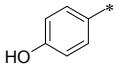	-H	0.41	NI	20.94
A16	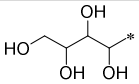	-H	NI	NI	NI
A17	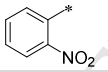	-H	NI	30.64	27.42
A18	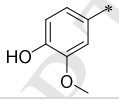	-H	9.01	NI	17.08
A19	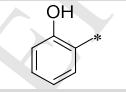	-H	97.87 [31.50]	24.1	86.07
A20	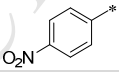	-H	NI	19.02	40.08
A21	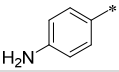	-H	NI	38.64	NI
A22	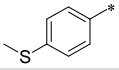	-H	82.59 [44.36]	34.11	89.33 [2.58]
A23	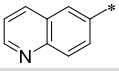	-H	84.23 [34.37]	36.01	53.77
A24	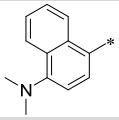	-H	6.33	58.31	8.05
A25	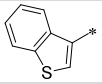	-H	3.57	24.42	24.34
A26		-H	17.26	8.28	24.89

A27	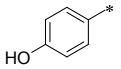	-CH_3	NI	23.94	36.97
A28	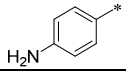	-CH_3	NI	9.54	51.82
PEN	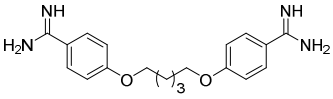		[0.0016]	N/A	N/A
BZD	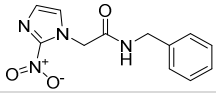		N/A	N/A	[2.4]
MIL	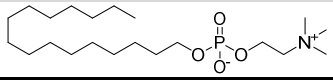		N/A	[2.51]	N/A

[a] Standard deviation is within ±10% of each value.

[b] % of cell growth inhibition and EC_{50} were determined as the median of at least two independent experiments

NI, No Inhibition at 50 µM.

N/A, Not Available

Whereas the first library of thiosemicarbazone (**A1-14**) was characterized by a high lipophilic aromatic portion (with the only exception of **A6**), in the second library we opted for more polar substituents. In particular hydroxyl (**A15-16,18-19,21,27**), nitro (**A17,20**) or amino groups (**A21,28**) were preferred with the aim to obtain molecules with higher hydrophilicity and water solubility and to study how these previously unexplored substituents could affect activity. Compound **A8** was the only heterocyclic derivative of the first series, therefore in the second library we extended the structure-activity relationship toward other heterocyclic or extended benzofused systems such as thiophene (**A26**), benzothiophene (**A25**), naphthalene (**A24**) or quinolone (**A23**) ring (Figure 3).

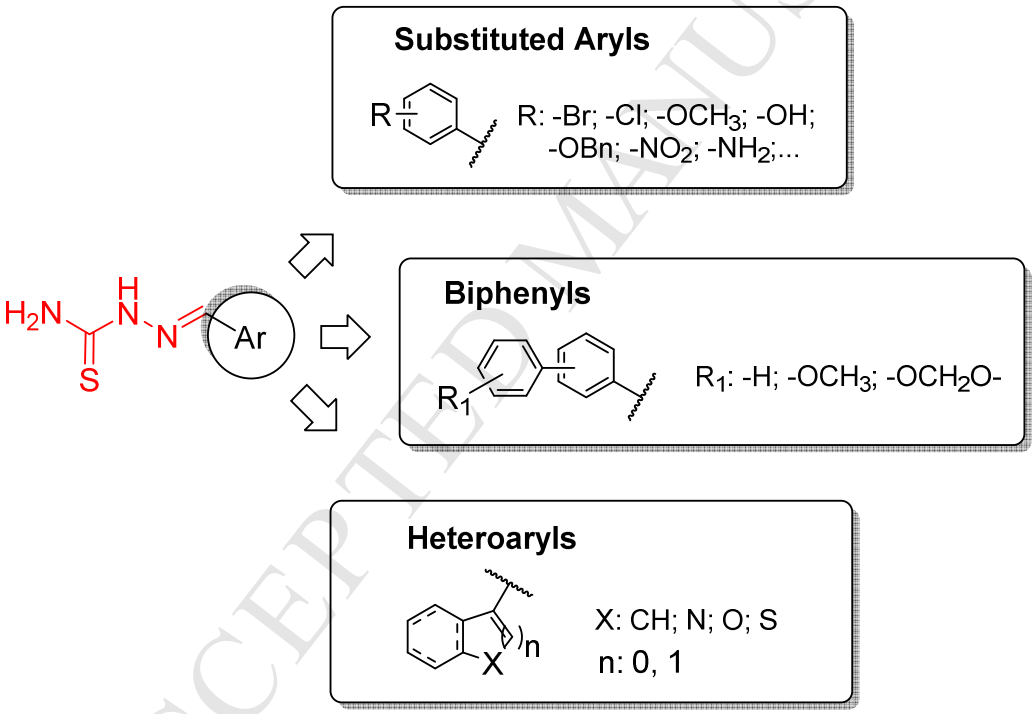

Figure 3. General structure of the thiosemicarbazones studied in the present paper.

The thiosemicarbazones **A1-28** were obtained in high yield (65-95% yield) and purity (>95%) through condensation between the appropriate carbonyl compound and thiosemicarbazide in 50% aqueous ethanol at 60° for 2-12 hours (Scheme 1). Thiosemicarbazones **A1-9** and **A15-28** were prepared starting from the respective carbonyl compounds commercially available. For the

synthesis of thiosemicarbazones **A10**-**14** the proper benzaldehydes employed as starting materials were synthesized as previously described. [31]

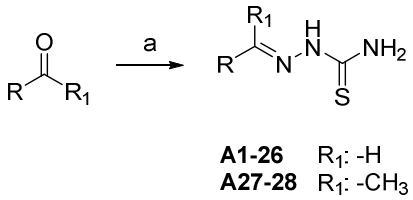

Scheme 1. General procedure for the synthesis of thiosemicarbazones **A1**-**A28**. Reagents and conditions: a) thiosemicarbazide (1 eq.), EtOH:H_2O 1:1, 60°C, 2-12h, 85-95 % yield.

2.2. *In vitro* anti-parasitic screening

The synthesized thiosemicarbazones **A1**-**28** were evaluated for their *in vitro* anti-parasitic activities against cultured bloodstream form of *T. brucei* and the intracellular amastigote stage of *L. infantum* and *T. cruzi* with all tests being performed using phenotypic screening approaches. The library here presented was part of a larger phenotypic screening campaign including different compounds libraries. [13] The anti-parasitic potential of this class of compound was represented as percentage of parasitic cell growth inhibition at 50 μM (Table 1 and Figure SI-1) and compounds associated with anti-parasitic activity >80% at 50 μM, were further evaluated in dose-response studies to determine their EC_{50} values.

The *T. brucei* assay relies on indirect determination of parasite numbers by quantification of total DNA released from cells present in the wells of plates using the SYBR Green I DNA fluorescent dye. PEN was used as reference compound exhibiting an EC_{50} of 1.6 nM±0.2, which is comparable with the value reported in literature. [32] Eight compounds (**A2**, **A6**, **A9**, **A12**, **A14**, **A19** and **A22**-**23**) yielded anti-parasitic activity against *T. brucei* > 80% at 50 μM, and in dose-response studies, these were associated with EC_{50} values in the μM range (2.31 - 44.68 μM, Table 1) with **A12** (EC_{50} = 7.45 μM) and **A14** (EC_{50} = 2.31 μM) being the most potent trypanocidal agents of the series. In

addition, we evaluated the anti-parasitic activity against the amastigote stage of *T.cruzi*, which is a more physiological and disease-relevant model than those assays that rely on insect stages or axenic amastigote screens. In the *T. cruzi* assay, the osteosarcoma human U2OS cell-line was infected with trypomastigote forms of the Y strain of *T. cruzi* in the presence of compounds. Infected cells were incubated for 72 h prior to fixation, staining and quantification of antiparasitic activity by image analysis. BZD was used as reference, exhibiting an EC_{50} of 2.4 μM, which is comparable with the value reported in literature. [33] Eight compounds (**A1**-**2**, **A8**-**10**, **A12**, **A14** and **A22**) were able to reduce infection by at least 80% at 50 μM and the EC_{50} for these were determined. With the exception of **A2** (EC_{50} = 15 μM) and **A12** (EC_{50} = 29.5 μM), the other six thiosemicarbazones ((**A1**, **A8** - **A10**, **A14**, **A22**) showed EC_{50} in the low micromolar range between 1.31 μM and 4.17 μM, thus giving the most potent anti-*T. cruzi* compounds in the series and revealing a comparable or higher activity than the reference drug BDZ (EC_{50} = 2.4 μM). All the synthesized compounds were also screened against intracellular amastigote stage of *L.infantum*, infecting a human leukemic monocyte cell line THP-1. MIL and AmpB were utilized as positive controls yielding EC_{50} of 2.51 μM and 0.2 μM, respectively. Notwithstanding the promising anti-trypanosomatidic activity against *T. brucei* and *T. cruzi,* almost all the tested compounds yielded low efficacy against the intracellular amastigote stage of *L. infantum,* with a percentage of cell growth inhibition <40% at 50 μM. The only exception to this was **A14,** which yielded an EC_{50} of 6.14 μM, being comparable with the antileishmanial activity with MIL (EC_{50} of 2.51 μM).

Focusing on the anti-parasitic activity profile of the most active compounds in the series, compounds **A1**, **A8** and **A10** were potent and selective anti-*T. cruzi* agents (EC_{50} = 2.29 μM, 1.87 μM and 4.17 μM, respectively). Compounds **A9** and **A22** were active against *T. cruzi* (EC_{50} = 1.59 μM and EC_{50} = 2.58 μM, respectively), preserving modest anti-parasitic activity against *T. brucei* (EC_{50} = 16.88 μM and EC_{50} = 44.36 μM, respectively), whereas, **A12** resulted four-fold more active against *T. brucei* (EC_{50} = 7.95 μM) than *T. cruzi* (EC_{50} = 29.5 μM). The most promising result was achieved with **A14,** which exibited single digit μM potency and comparable anti-parasitic activity

against all the three parasitic species (*Tb*EC_{50} = 2.31 μM; *Li*EC_{50} = 6.14 μM; *Tc*EC_{50} = 1.31 μM), thus showing a pan-anti-trypanosamatidic activity profile. Comparing the anti-parasitic activity of the thiadiazole **B1**-**14** with the respective thiosemicarbazones **A1**-**14**, the latter exhibited a better or comparable overall anti-parasitic profile. It is worth mentioning that the activity of the thiadiazoles **B1**-**14** (compared with **A1**-**A14**) against *T .brucei* and *L. infantum* was already described in our previous study, [31], whereas here we report for the first time the anti-parasitic evaluation against *T. cruzi* (Table SI-1).

All the synthesized thiosemicarbazones **A1**-**A28** were also evaluated for their inhibition of *Lm*PTR1 and *Tb*PTR1 enzymes. Compound **A6** inhibited *Lm*PTR1 with 56.45±0.86 % at 50 μM, whereas all the other compounds showed <40 % inhibition at 50 μM, (Table SI-2) suggesting that these compounds may inhibit different targets in the parasite. Therefore, in the present work we mainly focused on the phenotypic antiparasitic activity of this library of synthesized compounds. The investigation of the mechanism of action of the most active candidates will be part of further studies.

2.3. Potentiation of the trypanocidal activity of MTX by combination with thiosemicarbazones.

Combination of multiple trypanocidal agents is considered one important option in anti-parasitic therapy. In our previous work, we estimated and subsequently confirmed the importance of the combined biological effect, in terms of gain in potency and reduction of toxicity, resulting from simultaneous administration of two trypanocidal agents. [14, 26] It has been reported that in trypanosomatids, MTX (a DHFR inhibitor) anti-parasitic activity is potentiated in combination with other anti-trypanocidal agents by a multi-target inhibition. [14, 26] Therefore, thiosemicarbazones were assayed in combination with MTX against *T. brucei* in order to assess the trypanocidal potentiation effect by a preliminary assay of all compounds and a deeper analysis using the Combination Index methods for the most potent inhibitors. Preliminary combination experiments in *T. brucei* were conducted with compounds **A1**-**28** at 10 μM as a single agent, arbitrarily selected,

and in combination with 4 µM MTX (MTX EC_{30} against *T. brucei*) [14]; the anti-parasitic activity was expressed as % cell growth inhibition and is reported in Figure 4A. The potency of combination was estimated through determination of a Potentiating Index (PI) given by % inhibition of the combination/(% inhibition of the compound + % inhibition of 4 µM MTX). PI reflects the capacity of the compounds to increase the anti-parasitic activity of MTX beyond what would be expected by the simple addition of the individual effects (Figure 4A and Table-SI-3) at a fixed ratio. A potentiating effect is observed for PI higher than 1.

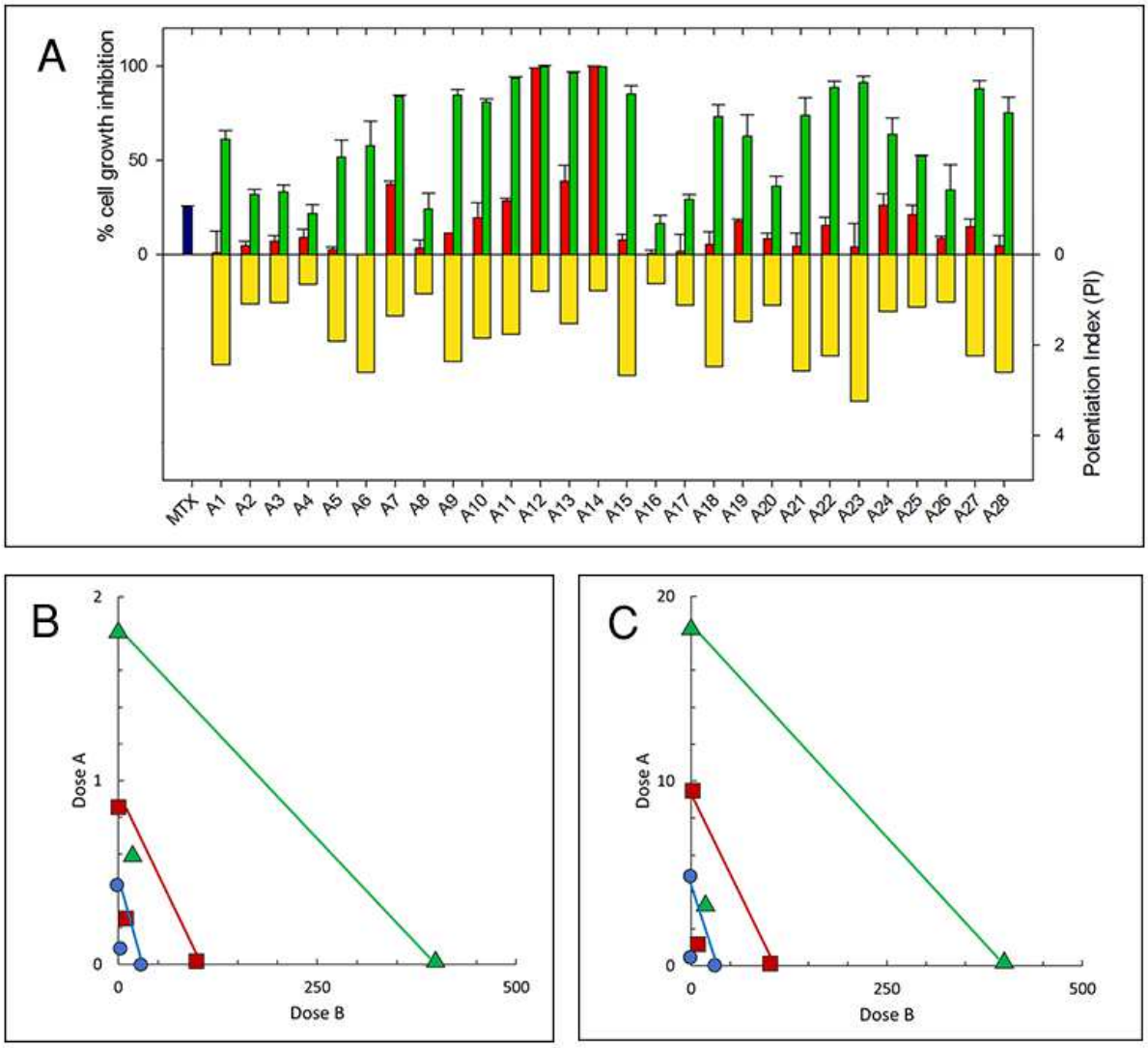

Figure 4. A) Anti-parasitic activity against *T. brucei* of compounds **A1-28** tested as single agent at

10 μM (in red) and in combination with 4 μM of MTX (in green). The anti-parasitic activity of MTX as single agent at 4 μM is reported in blue bar. As a quantitative measure of potentiation, a PI of the combination was determined (yellow bar). **B)** Compusyn generated isobologram of the combination between MTX (Dose B) and compound **A12** (Dose A). Fraction affected (Fa) = 0.3 is shown in blue (circle), Fa = 0.4 in red (square) and Fa = 0.5 in green (triangle). Measurement unit axes = μM. **C)** Compusyn generated isobologram of the combination between MTX (Dose B) and compound **A14** (Dose A). Fa = 0.5 is shown in blue (circle), Fa = 0.75 in red (square) and Fa = 0.9 in green (triangle). Measurement unit axes = μM. Fa = fraction affected. Fa=1 means 100 % parasite growth inhibition; Fa = 0.5 means 50 % parasite growth inhibition (*i.e.* EC_{50}).

Thirteen compounds were able to potentiate the activity of MTX with PI>2.00 (**A1**, **A6**, **A9**, **A15**, **A18**, **A21-23**, **A27-28**). As **A12** and **A14** resulted the most active compounds as single agents against *T. brucei*, we employed the Compusyn software to further evaluate the gain in potency of the combination with MTX. Basing on the EC_{50} values of **A12**, **A14** and MTX (EC_{50} **A12** = 4.72 μM; EC_{50} **A14** = 0.44 μM; EC_{50} MTX = 22.7 μM) a constant ratio between the concentrations of the two compounds and MTX was set as follows: **A12** (molar ratio of 1:6) and **A14** (molar ratio of 1:30). [34] This enabled us to quantify synergism between the two compounds (Combination Index, CI) and to determine the dose reduction (Dose Reduction Index, DRI) needed to observe the effect in combination and with the selected dose of each compound alone. MTX at its EC_{30} was combined with compounds **A12** and **A14** at their EC_{50}. The combination showed a CI of 0.28 and 0.41 respectively (Table 2). Where CI is <1, the combination can be considered synergistic, therefore the observed CIs show strong synergism. The isobolograms for the combination of compounds **A12** and **A14** with MTX are shown in Figure 4B-C and for compound **A12** the EC_{50} determined for the combination showing CI of 0.28 was 4.16 μM. This enabled an average DRI at the EC_{50} of 6.36 for MTX (EC_{50} MTX = 3.6 μM) and of 7.94 for **A12** (EC_{50} **A12** = 0.59 μM) (Figure 4B and Table 2). Regarding compound **A14**, for a CI of 0.41 we observed an EC_{50} of 3.58 μM resulting in a DRI for

MTX at the EC_{50} of 6.56 (EC_{50} MTX = 3.5 μM) and a DRI for **A14** of 3.84 (EC_{50} **A14** = 0.11 μM) (Figure 4C and Table 2). The determination of the PI and the more detailed analysis through the Compusyn software demonstrated how the anti-parasitic activity of MTX can be potentiated in combination with thiosemicarbazones. Similar results were obtained with flavonoids. More studies will be performed to understand the molecular mechanism of the combination action.

Table 2. Compusyn software analysis for the activity of two-drugs combination with MTX and either **A12** (molar ratio of 6:1) or **A14** (molar ratio of 30:1), against the blood stream forms of *T. brucei*. The parameters m, D_m, and r are the slope, anti-log of the x-intercept, and the linear correlation coefficient of the median-effect plot, which signifies the shape of the dose-effect curve, the half maximal inhibitory concentration (IC_{50}), and the conformity of the data to the mass-action law, respectively. D_m and *m* values are used for calculating the CI (Combination Index) and DRI (Dose Reduction Index) values as described by Chou. [34]. CI values, CI<1, CI=1 and CI>1 represent synergism, additive effect and antagonism respectively.

	***D_m* (μM)**	***m***	***R***	**CI (at EC_{50})**	**DRI for MTX (at EC_{50})**	**DRI for A12 and A14 (at EC50)**	**EC_{50} (μM)**
MTX	22.74	0.76	0.99	--	--	--	22.74
A12	4.72	1.63	0.86	--	--	--	4.72
A14	0.44	1.34	0.92	--	--	--	0.44
MTX + **A12** (6:1)	4.16	1.42	0.98	0.28	6.36	7.94	3.60 (MTX) 0.59 (**A12**)
MTX + **A14** (30:1)	3.58	1.34	0.97	0.41	6.56	3.84	3.50 (MTX) 0.11 (**A14**)

2.4. *In vitro* early-toxicity and selectivity against human A549 and WI-38 cell lines

Early-toxicity related issues for the synthesized compounds **A1**-**28** and reference drugs (*i.e.* PEN, Amp B, MIL and BZD) were determined using industry standard screening technologies. These studies included inhibition of *h*ERG, Aurora B and five cytochrome P450 isoforms (1A2, 2C9,

2C19, 2D6, 3A4), cytotoxicity against the A549 (human lung adenocarcinoma epithelial), and WI-38 (caucasian fibroblast-like fetal lung) cell-lines, mitochondrial toxicity in the 786-O (renal carcinoma) cell-line at a compound concentration of 10 µM with the results expressed as % inhibition (Table SI-4). The data were organized adopting a grid map system for rapid and intuitive visualization (Figure 5A).

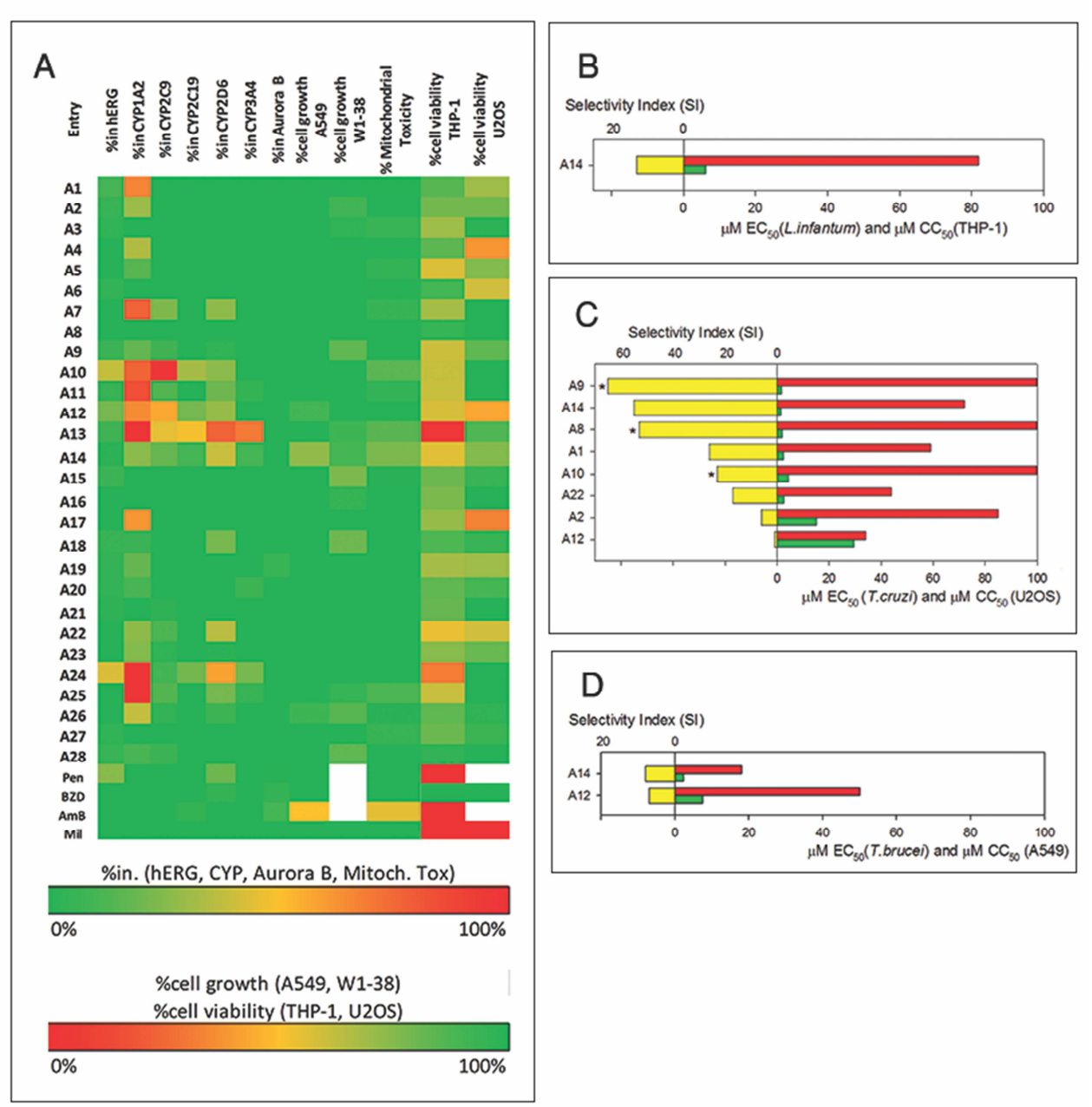

Figure 5. Biological activity profile of thiosemicarbazones. **A)** Grid map reporting data from *in vitro* assays to determine possible liability for all synthesized compounds. The compounds were

tested at 10 μM for *h*ERG, CYP isoforms, Aurora B, mitochondrial toxicity (Mitoch. Tox), A549 and W1-38 cell growth. The compounds were tested at 100 μM for THP-1 human macrophages viability and at 50 μM for U2OS cells viability. The percentages of each biological properties range from 0 % to 100 % and is shown in traffic light code from red to green. Green means a value within the the cut-off number for the specific properties, red means a value out of the cut-off number for the specific property. The ideal compound should have all the cells of the heat-map in green colour (**A20** or **A21** for example). For a white cell, the assays has not been performed. PEN, BZD, AmB and MIL are reported as reference compounds and properties for the mentioned standard drugs have been measured. **B, C, D.** Anti-parasitic activity expressed as EC_{50} (green bar) against *L. infantum* **(B),** *T. cruzi* (**C)** and *T. brucei* **(D)** compared with the CC_{50} (red bar) against THP-1 cells **(B),** U2OS cells **(C)** and A549 cells **(D)** for the most active thiosemicarbazones. The Selectivity Index (SI) was calculated as CC_{50}/EC_{50} (yellow bar). The SI highlighted with "*" is understimated due to the low toxicity of the compound. The data for all compounds are reported in SI Table SI-4, Table SI-5 and Table SI-6.

To reduce the liabilities of the compounds, a cut-off <30 % was set for acceptable mitochondrial toxicity, inhibition of *h*ERG and cytochrome P450 isoforms, whereas for A549/WI-38 cell growth, the cut-off >70 % was selected. The mentioned cut-off values have previously been selected for early phase inhibitors in order to progress to a further evaluation step in the drug discovery process. [14] Almost all evaluated thiosemicarbazones showed a safe toxicological profile against *h*ERG, cytochrome P450 isoforms and cell-lines. Nine compounds (**A1**, **A7**, **A10-13**, **A17** and **A24-25**) inhibited the 1A2 isoform of cytochrome P450 while compound **A13** interfered with all isoforms of cytochrome P450.

As the compounds were assayed against intracellular forms of *T. cruzi* and *L. infantum*, the toxicity and selectivity of the compounds against two human host cells (THP-1 and U2OS) was evaluated.

THP1 human macrophages are the host cells for amastigote *L. infantum*. The cytotoxicity at 100 μM was expressed as % cell viability (Figure 5A and Table SI-5) and the THP-1 CC_{50} (the concentration inducing a 50 % reduction of THP-1 cell growth) estimated. A Selectivity Index (SI) between human and parasitic cells was extrapolated as ratio between CC_{50} and EC_{50}, and for a compound to be considered non-toxic it should be at least 10. [35] Focusing in particular on **A14**, the only thiosemicarbazone with anti-leishmanial activity (*Li*EC_{50} = 6.14 μM), a THP-1 CC_{50} of 82 μM and a SI of 13 was calculated, revealing a safe profile with respect to human macrophages (Figure 5B). The toxicity against the U2OS cell-line, host for *T. cruzi*, was in addition determined and expressed in term of cell viability at 100 μM (Figure 5A and Table SI-5) and the U2OS cell-line CC_{50} and SI calculated as well. Thiosemicarbazones **A1, A8-10, A14** and **A22** were associated with the least host cell toxicity (CC_{50} >44 μM) beside a promising anti-parasitic activity (*Tc*EC_{50} < 4.17 μM), resulting in SI >17, with **A14** (*Tc*EC_{50} = 1.31 μM, CC_{50} = 72 μM, SI = 55) one of the most promising anti-*T.cruzi* compound. (Figure 5C). In contrast, **A2** (*Tc*EC_{50} = 15 μM, CC_{50} = 85 μM, SI = 6) and **A22** (*Tc*EC_{50} = 29.5 μM, CC_{50} = 34 μM, SI = 1) due to the low anti-*T. cruzi* activity resulted in low selective against the U2OS cell-line (SI < 10, Figure 5C). Finally, as *T. brucei* is an extracellular parasite, the anti-parasitic activity of the most active compounds against this strain was compared with the toxicity against the A549 cell-line. Thiosemicarbazones, **A12** (*Tb*EC_{50} = 7.45 μM; CC_{50} = 50 μM, SI = 7) and **A14** (*Tb*EC_{50} = 2.31 μM; CC_{50} = 18 μM, SI = 8) indicated borderline selectivity against *T. brucei* with the respect of human A549 cells (Figure 5D). Thus, the most promising anti-parasitic thiosemicarbazones possess an acceptable *in-vitro* early toxicity profile and selectivity against human cells, especially in the case of compounds active against *T. cruzi*, resulting in a suitable scaffold to be explored for further improved anti-parasitic agents. We also measured the early-tox profile of the drugs of reference (Figure 5A) for comparison with the synthesized compounds. The general early-tox properties were suitable for a drug-like profile (almost all the heat-map cells were green colored for PEN, BZD, AmB and MIL), while the EC_{50}

against the human cells THP-1 and U2OS were red colored, highlighting a potential toxicity and in some cases (MIL) yielded a SI < 10 (Table SI-6).

3. Conclusion

In the present work, we evaluated a library of aryl thiosemicarbazones as anti-trypanosomatid agents. All compounds were assayed as single agents against *T. brucei*, and intracellular amastigote *T. cruzi* and *L. infantum*. Eight thiadiazoles showed good anti-parasitic activity against *T. brucei* and other eight compounds resulted active against *T. cruzi*. The particularly interesting compounds were **A2**, **A9**, **A12**, **A19** and **A22** that exerted a dual trypanocidal activity against both *T. brucei* and *T. cruzi* and low cytotoxicity with the respect of human cells (*i.e.* THP-1, A549 and U2OS) showing an overall selectivity index >20. However, the compound library resulted in low activity against the intracellular amastigote stage of *L. infantum*. The noteworthy exception is represented by thiosemicarbazone **A14** that resulted in the highest degree of trypanocidal activity with comparable EC_{50} values against the three parasitic species (*Tb*EC_{50} = 2.31 μM; *Li*EC_{50} = 6.14 μM; *Tc*EC_{50} = 1.31 μM) and SI >10 with respect of human macrophages as well as a comparable activity/*in vitro* early-toxicity profile to BZD and MIL. These results lay the foundation for the development of dual or pan-anti-trypanosomatidic agents. However, the molecular target of thiosemicarbazones remains elusive. It is noteworthy that the *in vitro* early-toxicity studies related to all synthesized compounds suggested that most of the compounds have a safe profile, in some cases better than for the drug in use. Almost all thiosemicarbazones were able to potentiate the anti-*T. brucei* activity of MTX in combination, and for compounds **A12** and **A14** the synergistic effect between the two molecules was quantified by Compusyn software. The thiosemicarbazone are a suitable chemical scaffold for the development of anti-parasitic drugs and further chemical modification, together with a full understanding of their molecular target, could allow to exploit their anti-parasitic potential.

4. Experimental section

4.1. Synthetic procedures

All commercially available chemicals and solvents were reagent grade and were used without further purification unless otherwise specified. Reactions were monitored by thin-layer chromatography on silica gel plates (60F-254, E. Merck) and visualized with UV light, iodine vapours, cerium ammonium sulfate or alkaline $KMnO_4$ aqueous solution. The following solvents and reagents have been abbreviated: tetrahydrofuran (THF), ethyl ether (Et_2O), dimethyl sulfoxide (DMSO), ethyl acetate (EtOAc), dichloromethane (DCM), dimethyl formamide (DMF), methanol (MeOH), formic acid (FA) and acetonitrile (ACN). All reactions were carried out with standard techniques or under microwave irradiation. NMR spectra were recorded on a Bruker 400 spectrometer with ^{1}H at 400.134 MHz and ^{13}C at 100.62 MHz. Proton chemical shift was referenced to the TMS internal standard. Chemical shifts are reported in parts per million (ppm, δ units). Coupling constants are reported in units of Hertz (Hz). Splitting patterns are designed as s, singlet; d, doublet; t, triplet; q quartet; dd, double doublet; m, multiplet; b, broad. Mass spectra were obtained on a 6520 Accurate-Mass Q-TOF LC/MS and 6310A Ion TrapLC-MS(n). The melting point was recorded on a Stuart, SMP3 (Barloworld Scientific Limited Stone, Staffordshire, UK) and was uncorrected. The purity of the compounds was assessed by ^{1}H NMR and melting point resulting to be > 95%.

General procedure for the synthesis of aryl-thiosemicarbazone **A1**-**A28**. To a solution of the appropriate aldehyde or ketone (1 eq.) in 50% aqueous ethanol (v/v), thiosemicarbazide (1 eq.) was added. The mixture was stirred at 60°C for 2-12 hours, cooled at room temperature and diluted with water. The precipitate formed was collected and recrystallized from water and ethanol to give the desired product in 65-95 % yield.

(*E*)-2-(3-bromobenzylidene)hydrazinecarbothioamide (**A1**). White crystal (89% yield). ^{1}H-NMR (DMSO-d6) δ: 7.35 (t, 1H, CH_{Ar}, J=8.0); 7.56 (m,1H, CH_{Ar}); 7.69 (d, 1H, CH_{Ar}, J=7.6); 8.0 (1H, s, CH=N); 8.18 (t, 1H, CH_{Ar}, J=1.6); 8.19 (s, 1H, NH_2); 8.25 (s, 1H, NH_2); 11.5 (s, 1H, NH). ^{13}C-NMR (DMSO-d6) δ: 122.31; 126.93; 128.84; 130.65; 132.23; 136.66; 140.41; 178.16. mp [212.6-212.7°C]. HRMS m/z $[M+H]^+$ Calcd for $C_8H_8BrN_3S$: 257.9695, 259.9675. Found: 257.9705, 259.9672.

(*E*)-2-(2-methoxybenzylidene)hydrazinecarbothioamide (**A2**). White crystal (92% yield). ^{1}H-NMR (DMSO-d6) δ: 3.83 (s, 3H, CH_3); 6.95 (t, 1H, CH_{Ar}, J=7.2); 7.05 (d, 1H, CH_{Ar}, J=8.4); 7.37 (t,1H, CH_{Ar}, J=7.6); 7.93 (s, 1H, NH_2) 8.09 (d, 1H, CH_{Ar}, J=7.6); 8.13 (s, 1H, NH_2); 8.41(s, 1H, CH=N); 11.41 (s, 1H, NH). ^{13}C-NMR (DMSO-d6) δ: 56.13; 112.09; 120.99;122.64; 126.54; 131.74; 138.32; 158.20; 178.30. mp [206.4-206.5°C]. HRMS m/z $[M+H]^+$ Calcd for $C_9H_{11}N_3OS$: 210.0696. Found: 210.0694.

(*E*)-2-(3,4-dimethoxybenzylidene)hydrazinecarbothioamide (**A3**). White crystalline solid (74% yield). ^{1}H-NMR (DMSO-d6) δ:3.78 (s, 3H, CH_3); 3.82 (s, 3H, CH_3); 6.95 (d, 1H, CH_{Ar}, J=8.4); 7.14 (dd, 1H, CH_{Ar}, J=2.0, 8.4), 7.52 (d, 1H, CH_{Ar}, J=2.0); 7.97 (s, 1H, CH=N); 8.01 (s, 1H, NH_2); 8.15 (s, 1H, NH_2); 11.317 (s, 1H, NH). ^{13}C-NMR (DMSO-d6) δ: 55.97; 56.14; 108.98; 111.69; 122.61; 127.37; 142.98; 149.59; 151.05; 178.01. mp [193.2-193.4°C]. HRMS m/z $[M+H]^+$ Calcd for $C_{10}H_{13}N_3O_2S$: 240.3014. Found: 240.3016.

(*E*)-2-(2,6-dimethoxybenzylidene)hydrazinecarbothioamide (**A4**). White crystalline solid (83% yield). ^{1}H-NMR (DMSO-d6) δ:3.79 (s, 6H, CH_3); 6.69 (d, 2H, CH_{Ar}, J=8.4); 7.22 (s, 1H, NH_2); 7.31 (t, 1H, CH_{Ar}, J=8.4); 8.13 (s, 1H, NH_2); 8.31 (s, 1H, CH=N); 11.35 (s, 1H, NH). ^{13}C-NMR (DMSO-d6) δ: 55.97; 104.30; 110.49; 131.21; 138.21; 158.81;177.69. mp [190.1-190.2°C]. HRMS m/z $[M+H]^+$ Calcd for $C_{10}H_{13}N_3O_2S$: 240.0801. Found: 240.0803.

(*E*)-2-(3,4,5-trimethoxybenzylidene)hydrazinecarbothioamide (**A5**). White crystalline solid (71% yield). ^{1}H-NMR (DMSO-d6) δ:3.68 (s, 3H, CH_3); 3.83 (s, 6H, CH_3); 7.09 (s, 2H, CH_{Ar}); 7.95 (s, 1H, CH=N); 8.08 (s, 1H, NH_2); 8.22 (s, 1H, NH_2); 11.43 (s, 1H, NH). ^{13}C-NMR (DMSO-d6) δ: 56.04; 60.04; 104.59; 129.62; 138.99; 142.14; 153.10; 177.74. mp [198.0-198.1°C]. HRMS m/z $[M+H]^+$ Calcd for $C_{11}H_{15}N_3O_3S$: 270.0907. Found: 270.0911.

(*E*)-2-(3,4-dihydroxybenzylidene)hydrazinecarbothioamide (**A6**). Dark yellow crystalline solid (68% yield). ^{1}H-NMR (DMSO-d6) δ:6.76 (d, 1H, CH_{Ar}, J= 8.0); 7.02 (dd, 1H, CH_{Ar}, J= 1.2, 8.0) 7.18 (s, 1H, CH_{Ar}); 7.72 (s, 1H, NH_2); 7.89 (s, 1H, CH=N); 8.03 (s, 1H, NH_2); 8.99 (s, 1H, OH); 9.45 (s, 1H, OH): 11.20 (s, 1H, NH). ^{13}C-NMR (DMSO-d6) δ: 113.81; 115.49; 120.12; 125.52; 143.25; 145.48; 147.70; 177.33. mp [245.7.0-245.9°C]. HRMS m/z $[M+H]^+$ Calcd for $C_8H_9N_3O_2S$: 212.0488. Found: 212.0429.

(*E*)-2-(3,4-dichlorobenzylidene)hydrazinecarbothioamide (**A7**). Pale yellow crystalline solid (86% yield). ^{1}H-NMR (DMSO-d6) δ:7.62 (d, 1H, CH_{Ar}, J=8.4); 7.71 (dd, 1H, CH_{Ar}, J=2.0, 8.4); 7.99 (s, 1H, CH=N); 8.23 (d, 1H, CH_{Ar}, J=2.0); 8.24 (s, 1H, NH_2); 8.28 (s, 1H, NH_2); 11.55 (s, 1H, NH). ^{13}C-NMR (DMSO-d6) δ: 128.19; 128.63; 131.18; 132.24; 132.29; 135.56; 139.86; 178.71. mp [185.8-186.0°C]. HRMS m/z $[M+H]^+$ Calcd for $C_8H_7Cl_2N_3S$: 247.9811. Found: 247.9808.

(*E*)-2-(furan-2-ylmethylene)hydrazinecarbothioamide (**A8**). Brown solid (65% yield). ^{1}H-NMR (DMSO-d6) δ: 6.61 (dd, 1H, CH_{Ar}, J=1.6, 3.2); 6.96 (d, 1H, CH_{Ar}, J=3.6); 7.61 (s, 1H, NH_2); 7.80 (d, 1H, CH_{Ar}, J=1.6); 7.97 (s, 1H, CH=N); 8.20 (s, 1H, NH_2); 11.42 (s, 1H, NH). ^{13}C-NMR (DMSO-d6) δ: 112.27; 112.78; 132.51; 144.91; 149.32; 177.73. mp [154.7-154.9°C]. HRMS m/z $[M+H]^+$ Calcd for $C_6H_7N_3OS$: 170.0383. Found: 170.0388.

(*E*)-2-((E)-3-phenylallylidene)hydrazinecarbothioamide (**A9**). Yellow crystalline solid (73% yield). ^{1}H-NMR (DMSO-d6) δ:6.86 (dd, 1H, CH, J=9.2, 16.0); 7.01 (d, 1H, CH, J=16.0); 7.31 (m, 1H, CH_{Ar}); 7.38 (t, 2H, CH_{Ar}, J=7.6); 7.55 (d, 2H, CH_{Ar}, J=7.6); 7.60 (s, 1H, NH_2); 7.90 (d, 1H CH=N, J=9.2); 8.17 (s, 1H, NH_2); 11.39 (s, 1H, NH). ^{13}C-NMR (DMSO-d6) δ: 125.03; 126.89; 128.79; 128.85; 135.85; 138.81; 144.67; 177.69. mp [190.0-190.1°C]. HRMS m/z $[M+H]^+$ Calcd for $C_{10}H_{11}N_3S$: 206.0747. Found: 206.0747.

(*E*)-2-([1,1'-biphenyl]-4-ylmethylene)hydrazinecarbothioamide (**A10**). Pale yellow solid (70% yield). ^{1}H-NMR (DMSO-d6) δ:7.36 (t, 1H, CH_{Ar}, J=7.2); 7.48 (t, 2H, CH_{Ar}, J=8.0); 7.72 (m, 4H, CH_{Ar}); 7.89 (d, 1H, CH_{Ar}, J=8.4); 8.04(s, 1H, NH_2); 8.09 (s, 1H, CH=N); 8.21 (s, 1H, NH_2); 11.46 (s, 1H, NH). ^{13}C-NMR (DMSO-d6) δ: 126.64; 126.82; 127.78; 127.87; 128.97; 133.31; 139.35; 141.25; 141.78; 177.94. mp [209.2-209.4°C]. HRMS m/z $[M+H]^+$ Calcd for $C_{14}H_{13}N_3S$: 256.0903. Found: 256.0905.

(*E*)-2-([1,1'-biphenyl]-3-ylmethylene)hydrazinecarbothioamide (**A11**). White solid (67% yield). ^{1}H-NMR (DMSO-d6) δ:7.39 (m, 1H, CH_{Ar}); 7.49 (m; 3H; CH_{Ar}); 7.69 (m; 1H; CH_{Ar}); 7.74 (m; 3H; CH_{Ar}); 8.13 (m; 3H; CH=N, CH_{Ar}, NH_2); 8.22 (s, 1H, NH_2); 11.47 (s, 1H, NH). ^{13}C-NMR (DMSO-d6) δ: 125.00; 126.77; 126.92; 127.71; 128.12; 128.92; 129.31; 134.88; 139.57; 140.65; 142.27; 178.05. mp [203.5-203.6°C]. HRMS m/z $[M+H]^+$ Calcd for $C_{14}H_{13}N_3S$: 256.0903 . Found: 2256.0901.

(*E*)-2-((3',4'-dimethoxy-[1,1'-biphenyl]-3-yl)methylene)hydrazinecarbothioamide (**A12**). Pale yellow solid (72% yield). ^{1}H-NMR (DMSO-d6) δ: 3.80 (s, 3H, CH_3); 3.86 (s, 3H, CH_3); 7.04 (d, 1H, CH_{Ar}, J= 8.8); 7.27 (m, 2H, CH_{Ar}); 7.46 (t, 1H, CHAr, J=7.6); 7.67 (d, 1H, CH_{Ar}, J=8.4); 7.72 (d, 1H, CH_{Ar}, J=7.6); 8.06 (s, 1H, CH_{Ar}); 8.1 (s, 1H, NH_2); 8.11 (s, 1H, CH=N); 8.21 (s, 1H, NH_2); 11.48 (s, 1H, NH). ^{13}C-NMR (DMSO-d6) δ: 55.57; 55.63; 110.71; 112.12; 119.14; 124.83; 125.90;

127.84; 129.08; 132.31; 134.70; 140.60; 142.29; 148.70; 149.02; 178.00. mp [204.2-204.4°C]. HRMS m/z $[M+H]^+$ Calcd for $C_{16}H_{17}N_3O_2S$: 316.1114. Found: 316.1117.

(*E*)-2-(3-(benzo[d][1,3]dioxol-5-yl)benzylidene)hydrazine-1-carbothioamide (**A13**). White crystalline solid (90% yield).^{1}H NMR (400 MHz, DMSO-d6) δ: 6.05 (d, J = 13.6 Hz, 2H), 6.97 (dd, J = 8.1, 25.3 Hz, 1H), 7.04 – 7.11 (m, 1H), 7.23 (dd, J = 1.9, 8.1 Hz, 1H), 7.35 (d, J = 1.9 Hz, 1H), 7.44 (t, J = 7.7 Hz, 1H), 7.58 – 7.72 (m, 1H), 8.02 – 8.19 (m, 3H), 8.22 (s, 1H), 11.47 (s, 1H). ^{13}C NMR (101 MHz, DMSO) δ 101.63, 107.78, 109.05, 120.97, 125.04, 126.80, 128.26, 129.62, 134.21, 135.23, 140.73, 142.69, 147.47, 148.42, 178.48. mp [215.5-216.8°C]. HRMS m/z $[M+H]^+$ Calcd for $C_{15}H_{13}N_3O_2S$: 299.0728. Found: 299.0730.

(*E*)-2-(4-((3,4-dichlorobenzyl)oxy)benzylidene)hydrazinecarbothioamide (**A14**). Pale yellow solid (80% yield). ^{1}H-NMR (DMSO-d6) δ: 5.17 (s, 2H, CH_2); 7.04 (d, 2H, CH_{Ar}, J=8.8); 7.45 (dd, 1H, CH_{Ar}, J=2.0, 8.4);7.65 (d, 1H, CH_{Ar}, J=8.4); 7.73 (d, 1H, CHAr, J=2); 7.75 (d, 2H, CHAr, J=8.8); 7.92 (s, 1H, NH_2); 7.99 (s, 1H, CH=N); 8.11(s, 1H, NH_2); 11.32 (s, 1H, NH). ^{13}C-NMR (DMSO-d6) δ: 67.71; 115.00; 127.24; 127.83; 128.90; 129.49; 130.40; 130.67; 131.09; 138.04; 141.99; 159.29; 177.65. mp [189.5-189.6°C]. HRMS m/z $[M+H]^+$ Calcd for $C_{15}H_{13}Cl_2N_3OS$: 354.0229. Found: 354.0226.

(*E*)-2-(4-hydroxybenzylidene)hydrazinecarbothioamide (**A15**). White solid (66% yield). ^{1}H-NMR (DMSO-d6) δ:6.78(d, 2H, CH_{Ar}, J=8.8); 7.61 (d, 2H, CH_{Ar}, J=8.8); 7.81 (s, 1H, NH_2); 7.95 (s, 1H, CH=N); 8.05 (s, 1H, NH_2); 9.85 (s, 1H, OH); 11.24 (s, 1H, NH). ^{13}C-NMR (DMSO-d6) δ: 115.50; 125.11; 129.00; 142.66; 159.21; 177.42. mp [229.8-230.1°C]. HRMS m/z $[M+H]^+$ Calcd for $C_8H_9N_3OS$: 196.0539. Found: 196.0540.

(*E*)-2-(2,3,4,5-tetrahydroxypentylidene)hydrazinecarbothioamide (**A16**). White crystalline solid (90% yield). ^{1}H NMR (400 MHz, DMSO-d_6) δ: 3.12 – 3.58 (m, 3H, CH), 3.74 (ddd, 1H, CH_2, *J* = 5.4, 6.6, 12.1), 3.84 (d, 1H, OH, *J* = 5.0), 4.00 (td, 1H, CH, *J* = 5.0, 6.9), 4.10 (d, 1H, OH, *J* = 4.9 Hz), 4.80 (t, 1H, OH, *J* = 5.5 Hz), 5.57 (d,1H, OH *J* = 4.9), 7.75 (s, 2H, NH_2), 7.94 (d, 1H, =CH, *J* = 7.0), 11.29 (s, 1H, NH). ^{13}C-NMR (DMSO-d6) δ: 66.8; 69.47; 71.08; 77.13; 91.65; 181.72. mp [181.5-181.7°C]. HRMS m/z $[M+H]^+$ Calcd for $C_6H_{13}N_3O_4S$: 224.0700. Found: 224.0701.

(*E*)-2-(2-nitrobenzylidene)hydrazinecarbothioamide (**A17**). Yellow solid (65% yield). ^{1}H-NMR (DMSO-d6) δ:7.62 (t, 1H, CH_{Ar}, J=8.4); 7.73 (t, 1H, CH_{Ar}, J=7.6); 8.01 (d, 1H, CH_{Ar}, J=8.4); 8.10 (s, 1H, NH_2); 8.37 (s, 1H, NH_2); 8.42 (d, 1H, CH_{Ar}, J=8.0); 8.46 (s, 1H, CH=N); 11.73 (s, 1H, NH). ^{13}C-NMR (DMSO-d6) δ: 124.43; 128.27; 128.37; 130.28; 133.26; 137.16; 148.23; 178.46. mp [254.8-255.0°C]. HRMS m/z $[M+H]^+$ Calcd for $C_8H_8N_4O_2S$: 225.0441. Found: 225.0444.

(*E*)-2-(4-hydroxy-3-methoxybenzylidene)hydrazinecarbothioamide (**A18**). White crystalline solid (84% yield). ^{1}H-NMR (DMSO-d6) δ: 3.82 (s, 3H, CH_3); 6.77 (d, 2H, CH_{Ar}, J=8.0); 7.03 (dd, 1H, CH_{Ar}, J=1.6, 8.0); 7.47 (d, 2H, CHAr, J=2.0); 7.93 (s, 1H, CH=N); 7.94 (s, 1H, NH_2); 8.10 (s, 1H, NH_2); 9.43 (s, 1H, OH); 11.25 (s, 1H, NH). ^{13}C-NMR (DMSO-d6) δ: 56.22; 109.77; 115.66; 122.79; 126.04; 143.35; 148.54; 149.25; 177.85. mp [194.8-195.0°C]. HRMS m/z $[M+H]^+$ Calcd for $C_9H_{11}N_3O_2S$: 226.0645. Found: 226.0649.

(*E*)-2-(2-hydroxybenzylidene)hydrazinecarbothioamide (**A19**). White crystalline solid (76% yield). ^{1}H-NMR (DMSO-d6) δ:6.81 (t, 1H, CH_{Ar}, J=7.6); 6.86 (d, 2H, CH_{Ar}, J=8.0); 7.2 (m, 1H, CH_{Ar}); 7.9 (d, 2H, NH_2, CH_{Ar}, J=7.2); 8.09 (s, 1H, NH_2); 8.37 (s, 1H, CH=N); 9.86 (s, 1H, OH); 11.36 (s, 1H, NH). ^{13}C-NMR (DMSO-d6) δ: 116.00; 119.23; 120.30; 126.73; 131.05; 139.65; 156.36; 177.64. mp [229.8-230.0°C]. HRMS m/z $[M+H]^+$ Calcd for $C_8H_9N_3OS$: 196.0539. Found: 196.0541.

(*E*)-2-(4-nitrobenzylidene)hydrazinecarbothioamide (**A20**). Yellow crystalline solid (69% yield). ^{1}H-NMR (DMSO-d6) δ:8.09 (d, 2H, CH_{Ar}, J=8.8); 8.12 (s, 1H, CH=N); 8.22 (d, 2H, CH_{Ar}, J=8.8); 8.25(s, 1H, NH_2); 8.39 (s, 1H, NH_2); 11.70 (s, 1H, NH). ^{13}C-NMR (DMSO-d6) δ: 124.22; 128.61; 139.98; 141.19; 148.03; 178.96. mp [224.9-225.1°C]. HRMS m/z $[M+H]^+$ Calcd for $C_8H_8N_4O_2S$: 225.0441. Found: 225.0442.

(*E*)-2-(4-aminobenzylidene)hydrazinecarbothioamide (**A21**). Dark yellow crystalline solid (66% yield). ^{1}H-NMR (DMSO-d6) δ:5.58 (s, 2H, NH_2); 6.55 (d, 2H, CH_{Ar}, J=8.8); 7.42 (d, 2H, CH_{Ar}, J=8.8); 7.68 (s, 1H, NH_2); 7.87 (s, 1H, CH=N); 7.94 (s, 1H, NH_2); 11.10 (s, 1H, NH). ^{13}C-NMR (DMSO-d6) δ: 113.92; 121.74; 129.28; 144.13; 151.33; 177.38. mp [198.4-198.6°C]. HRMS m/z $[M+H]^+$ Calcd for $C_8H_{10}N_4S$: 195.0699. Found: 195.0697.

(*E*)-2-(4-(methylthio)benzylidene)hydrazinecarbothioamide (**A22**). Pale yellow solid (92% yield). ^{1}H-NMR (DMSO-d6) δ:2.5 (s, 3H, SCH_3); 7.26 (d, 2H, CH_{Ar}, J= 8.4); 7.73 (d, 2H, CHAr, J=8.4); 7.97 (s, 1H, NH_2); 8.01 (s, 1H, CH=N); 8.17 (s, 1H, NH_2); 11.40 (s, 1H, NH). ^{13}C-NMR (DMSO-d6) δ: 14.27; 125.47; 127.67; 130.61; 140.60; 141.86; 177.77. mp [199.7-199.9°C]. HRMS m/z $[M+H]^+$ Calcd for $C_9H_{11}N_3S_2$: 226.0467. Found: 226.0465.

(*E*)-2-(quinolin-6-ylmethylene)hydrazinecarbothioamide (**A23**). White crystalline solid (86% yield). ^{1}H-NMR (DMSO-d6) δ:7.53 (dd, 1H, CH_{Ar}, J=4.0, 8.0); 7.98 (d, 2H, CH_{Ar}, J=8.8); 8.16 (m, 2H, CH_{Ar}, NH_2); 8.25 (s, 1H, CH=N); 8.35 (m, 2H, CH_{Ar}, NH_2); 8.42(dd, 1H, CH_{Ar}, J=2.0, 9.2); 11.60 (s, 1H, NH). ^{13}C-NMR (DMSO-d6) δ: 122.00; 126.72; 127.84; 128.66; 129.26; 132.49; 136.20; 141.46; 148.37; 151.03; 178.13. mp [235.6-235.7°C]. HRMS m/z $[M+H]^+$ Calcd for $C_{11}H_{10}N_4S$: 231.0699. Found: 231.0702.

(*E*)-2-((4-(dimethylamino)naphthalen-1-yl)methylene)hydrazinecarbothioamide (**A24**). Pale yellow solid (69% yield). ^{1}H-NMR (DMSO-d6) δ:2.87 (s, 6H, CH_3); 7.11 (d, 1H, CH_{Ar}, J=8.0); 7.56 (t, 1H, CH_{Ar}, J=6.8); 7.62 (t, 1H, CH_{Ar}, J=6.8); 7.84 (s, 1H, NH_2); 8.04 (d, 1H, CH_{Ar}, J=8.0); 8.19 (m, 2H, CH_{Ar}, NH_2); 8.43 (d, 1H, CH_{Ar}, J=8.4); 8.79 (s, 1H, CH=N); 11.34 (s, 1H, NH). ^{13}C-NMR (DMSO-d6) δ: 44.55; 113.37; 123.13; 123.65; 124.78; 125.13; 127.03; 127.12; 127.60; 131.79; 141.99; 152.57; 177.47. mp [170.9-171.1°C]. HRMS m/z $[M+H]^+$ Calcd for $C_{14}H_{16}N_4S$: 273.1169. Found: 273.1169.

(*E*)-2-(benzo[b]thiophen-3-ylmethylene)hydrazinecarbothioamide (**A25**). Dark yellow solid (75% yield). ^{1}H-NMR (DMSO-d6) δ:7.47 (m, 2H, CH_{Ar}); 7.68 (s, 1H, NH_2); 8.03 (d, 1H, CH_{Ar}, J= 7.6); 8.24(s, 1H, CH_{Ar}); 8.29 (s, 1H, NH_2); 8.41 (s, 1H, CH=N); 8.58 (d, 1H, CH_{Ar}, J=7.6); 11.42 (s, 1H, NH). ^{13}C-NMR (DMSO-d6) δ: 123.34, 125.30; 125.75; 125.77, 130.93, 133.00; 135.83; 139.83; 140.41; 178.21. mp [233.6-233.8°C]. Calcd for $C_{10}H_9N_3S_2$: 236.0311. Found: 236.0314.

(*E*)-2-((3-methylthiophen-2-yl)methylene)hydrazinecarbothioamide (**A26**). Pale yellow solid (88% yield). ^{1}H-NMR (DMSO-d6) δ:2.87 (s, 3H, CH_3); 6.94 (d, 1H, CH_{Ar}, J= 5.2); 7.41 (s, 1H, NH_2); 7.54 (d, 1H, CH_{Ar}, J=4.8); 8.16 (s, 1H, NH_2); 8.35 (s, 1H, CH=N); 11.29 (s, 1H, NH). ^{13}C-NMR (DMSO-d6) δ: 14.11; 128.36; 131.35; 132.47; 137.65; 140.49; 177.76. mp [195.8-196.0°C]. HRMS m/z $[M+H]^+$ Calcd for $C_7H_9N_3S_2$: 200.0311. Found: 200.0315.

(*E*)-2-(1-(4-hydroxyphenyl)ethylidene)hydrazinecarbothioamide (**A27**). White crystalline solid (68% yield). ^{1}H-NMR (DMSO-d6) δ: 2.23 (s, 3H, CH_3); 6.75 (d, 2H, CH_{Ar}, J=8.8); 7.76 (d, 2H, CH_{Ar}, J=8.8); 7.81 (s, 1H, NH_2); 8.16 (s, 1H, NH_2); 9.75 (s, 1H, OH); 10.06 (s, 1H, NH). ^{13}C-NMR (DMSO-d6) δ: 13.85, 115.05, 128.25, 128.52, 148.36, 158.74, 178.55. mp [214.8-215.0°C]. HRMS m/z $[M+H]^+$ Calcd for $C_9H_{11}N_3OS$ 210.0696. Found: 210.0700.

(*E*)-2-(1-(4-aminophenyl)ethylidene)hydrazinecarbothioamide (**A28**). Pale yellow crystalline solid (84% yield). ^{1}H-NMR (DMSO-d6) δ:2.19 (s, 3H, CH_3); 5.49 (s, 2H, NH_2); 6.54 (d, 2H, CH_{Ar}, J=8.0); 7.62 (d, 2H, CH_{Ar}, J=7.6); 7.71 (s, 1H, NH_2); 8.08 (s, 1H, NH_2); 9.95 (s, 1H, NH). ^{13}C-NMR (DMSO-d6) δ: 14.02; 113.65; 125.20; 128.28; 149.43; 150.54; 178.58. mp [183.6-183.7°C]. HRMS m/z $[M+H]^+$ Calcd for $C_9H_{12}N_4S$: 209.0856. Found: 209.0859.

4.2. *In vitro* biological assays

4.2.1. Evaluation of activity against *L. infantum* intramacrophage amastigotes

Anti-parasitic activity against *L. infantum* intracellular amastigotes at 50 µM compound concentration was determined according to J. L. Siqueira-Neto *et al.* procedure with some modifications.[15] The Operetta high content automated imaging system (PerkinElmer) was used to acquire images and the Harmony Software (PerkinElmer) and was optimized quantifying host cells number, infection ratio and number of parasites per infected cell. After 72 h of incubation at 37 °C and 5% CO2, media was substituted by PBS. Macrophages were lysed by addition of 25 µL of Glo-lysis buffer (Promega). Steady-Glo reagent (Promega) was then added, and the content of each well was transferred to white-bottom 96-well plates. Luminescence intensity was read using a Synergy 2 multi-mode reader (Biotek). The ratio between infected cells and total number of cells is then calculated, and defined as the Infection Ratio (IR).[15]. All values reported correspond to the averages of the results obtained in at least two independent experiments.

4.2.2. Evaluation of activity against *T. brucei.*

Two different assays were employed in the determination of anti-*T. brucei* activity. The primary screening was performed with an indirect measurement of viability through quantification of trypanosome DNA with the cell-based SYBR Green assay, as previously described in the literature. [36] The activity of compounds was confirmed using a modified resazurin-based assay previously described in the literature. [37]. Concerning the resazurin assay *T. brucei* Lister 427 bloodstream

forms were grown at 37 °C, 5% CO_2, in complete HMI-9 medium, supplemented with 10% fetal calf serum (FCS) and 100 UI/mL of penicillin/streptomycin. Cultures were diluted until a cell density of 2 x 10^6/mL was reached. The efficacy of compounds against *T. brucei* bloodstream forms was evaluated using a modified resazurin-based assay previously described.[46] The compounds prepared from a stock solution in 10 mM DMSO and diluted in HMI-9 to 40 µM work solution (0.4% DMSO, with the DMSO limit in the assay being 0.4%). For EC_{50} determination 40 µM work solution was then used to perform serial dilutions (1:2) in a 96 well plate. For the potentiation assays, the mixtures were prepared using 10 µM test compound, (arbitrarily selected) and 4 µM MTX. For the combination analysis equipotent mixtures of MTX and **A12** and **A14** were used. Upon the compound addition to the test plate the mid-log bloodstream forms were added (100 µL) in complete HMI-9 medium at a final cell density of 1x10^4mL, in a final well volume of 200 µL with a maximum DMSO concentration of 0.2%. Following incubation for 72 hours at 37 °C 5% CO_2, 20 µL of a 0.5 mM resazurin solution was added and plates were incubated further for 4 hours under the same conditions. Fluorescence was measured at 540 nm and 620 nm excitation and emission wavelength, respectively, using a Synergy 2 Multi-Mode Reader (Biotek). The anti-trypanosomatid effect was evaluated by the determination of EC_{50} value (concentration required to inhibit growth by 50 %) and calculated by non-linear regression analysis using GraphPad Prism, Version 5.00 for Windows, GraphPad Software, San Diego California USA (www.graphpad.com). All values reported correspond to the averages of the results obtained in at least two independent experiments. The potentiation index (PI) was calculated using the formula: (activity of the combination / (activity of the compound + activity of 4 µM MTX)) (anti-parasitic activity of the compound + anti-parasitic activity of 4 µM MTX)). Compusyn software 1.0 was used to evaluate synergy. [34]. Pentamidine was used as the reference drug and internal control in all the assays. The average pentamidine EC_{50} for the assays was 1.60±0.20 nM.

4.2.3. Evaluation of activity against *T. cruzi*

The drug assay method consists of measuring compound activity on the U2OS (osteosarcoma) cell-line infected with *T. cruzi*, as described [33]. The U2OS cell-line, which presents a large cytoplasm that allow for improved quantification of *T. cruzi* amastigotes in high content analysis, was plated and allowed to grow as monolayer for 24 h prior to infection with tissue-derived trypomastigote forms of *T. cruzi*. Compounds were plated at a final concentration of either 50 µM (for single concentration screening) or variable concentrations (for dose-response tests) 24 h after infection. Infected cultures were exposed to compounds for 72 hours. Plates were processed for high content imaging and normalized compound activity was determined in relation to infected and non-infected controls. All values reported correspond to the averages of the results obtained in at least two independent experiments.

4.2.4. Cytotoxicity assessment against THP-1 macrophages and U2OS cells

The cytotoxicity of THP-1-derived macrophages was assessed by the colorimetric (3-(4,5-dimethylthiazol-2-yl)-2,5-diphenyl tetrazolium bromide (MTT) assay after 72 hours exposition to the compounds [14]. The cytotoxic effect in THP1 was evaluated by the determination of CC_{50} value (concentration required to inhibit growth by 50 %) and calculated by non-linear regression analysis using GraphPad Prism, Version 5.00 for Windows, GraphPad Software, San Diego California USA (www.graphpad.com). All values reported correspond to the averages of the results obtained in at least two independent experiments. The cytotoxicity against U2OS cells was determined from the anti-*T. cruzi* assay, based on the reduction of cell number in treated wells in comparison with infected, non-treated wells.

4.2.5. *h*ERG assay

This assay made use of Invitrogen's Predictor™ *h*ERG Fluorescence Polarisation Assay. The assay uses a membrane fraction containing *h*ERG channel (Predictor™ *h*ERG Membrane) and a high-affinity red fluorescent *h*ERG channel ligand, or "tracer" (Predictor™ *h*ERG Tracer Red), whose

displacement by test compounds can be determined in a homogenous, Fluorescence Polarization based format. [14] All experiments were performed in triplicate.

4.2.6. Cytochrome P450 1A2, 2C9, 2C19, 2D6 and 3A4 assays

These assays made use of the Promega P450-Glo™ assay platform. Each cytochrome P450 isoform assay made use of microsomal preparations of cytochromes from baculovirus infected insect cells. Action of the cytochrome P450 enzymes upon each substrate ultimately resulted in the generation of light and a decrease in this was indicative of inhibition of the enzymes. [14] All experiments were performed in triplicate.

4.2.7. Cytotoxicity assay against A549 and WI-38 cell-lines

The assays were performed using the Cell Titer-Glo® assay from Promega. The assay detects cellular ATP content with the amount of ATP being directly proportional to the number of cells present. The A549 cell-line was obtained from DSMZ (German Collection of Microorganisms and Cell Cultures, Braunschweig, Germany) and the WI-38 cell-line was obtained from ATCC (ATCC® CCL-75™) and were grown in DMEM with FCS (10 % v/v), streptomycin (100 μg/ml) and penicillin G (100 U/ml). [14] All experiments were performed in triplicate.

4.2.8. Aurora B kinase assay

This assay made use of the ADP-Glo Kinase Enzyme System from Promega which, which is a bioluminescent assay that employs firefly luciferase in a coupled-enzyme assay format to enable detection of ADP levels from ATPase assays. [14] All experiments were performed in triplicate.

4.2.9. Assessment of mitochondrial toxicity

This assay made use of MitoTracker® Red chloromethyl-X-rosamine (CMXRos) uptake and High Content Imaging to monitor compound mediated mitochondrial toxicity in the 786-O (renal carcinoma) cell line. Cells were maintained using RPMI-1640 medium containing 2 mM glutamine, FCS (10 % v/v), streptomycin (100 μg/ml) and penicillin G (100 U/ml). [14] All experiments were performed in triplicate.

ASSOCIATED CONTENT

Full data for the biological evaluation (enzyme inhibition for PTR1, antiparasitic activity and liability), are reported in the Supporting Information. This material is available free of charge via the Internet at http://pubs.acs.org. 1H-NMR and 13C-NMR spectra scan pictures for A1-A28 are available free of charge via the Internet at https://fp7h-synergy.h-its.org/data_files/299.

AUTHOR INFORMATION

Corresponding Author

*Prof. Maria Paola Costi, Dipartimento di Scienze della Vita, Università degli Studi di Modena e Reggio Emilia, Via Campi 103, 41125 Modena, Italia, Phone, 0039-059-205-8579; E-mail, mariapaola.costi@unimore.it.

Present Addresses

†Lucio H. Freitas-Junior, Division of Innovation, Instituto Butantan, São Paulo –SP, 05503-900, Brazil.

Author Contributions

The manuscript was written with contributions from all authors. All authors have given approval to the final version of the manuscript.

Funding Sources

This project has received funding from the European Union's Seventh Framework Programme for research, technological development and demonstration under grant agreement n° 603240 (NMTrypI - New Medicines for Trypanosomatidic Infections). We acknowledge the financial

support of the European Community's Seventh Framework Programme (FP7/2007-2013) and MIUR-PRIN2012 N° 2012 74BNKN_003 to MPC.

ACKNOWLEDGMENT

We acknowledge the COST Action CM1307 on "Targeted chemotherapy towards diseases caused by endoparasites", http://www.cost.eu/ COST_Actions/cmst/CM1307 for the contribution to the discussion of the research results.

ABBREVIATIONS

A549, human lung adenocarcinoma epithelial cell-line; ACN, acetonitrile; AmB, Amphotericin B; BZD, Benznidazole; CC_{50}, half maximal cytotoxicity concentration; CI, Combination Index; DCM, dichloromethane; DMF, dimethyl formamide; DMSO, dimethyl sulfoxide; DRI, Dose Reduction Index; EC_{50}, half maximal effective concentration; Et_2O, ethyl ether; EtOAc, ethyl acetate; Fa, Fraction affected; FA, formic acid; HAT, human African trypanosomiasis; IC_{50}, half maximal inhibitory concentration; IR, Infection Ratio; *L. donovani*, *Leishmania donovani*; *L. infantum*, *Leishmania infantum*; MeOH, methanol; MIL, miltefosine; MTX, methotrexate; MTT, dimethylthiazol-2-yl)-2,5-diphenyl tetrazolium bromide; PEN, Pentamidine; PI, Potentiation Index; SI, Selectivity Index; *T. brucei*, *Trypanosoma brucei*; *T. cruzi*, *Trypanosoma cruzi*; THF, tetrahydrofuran; THP1, human monocytic cell-line; WI-38, caucasian fibroblast-like fetal lung cell-line; 786-O, renal carcinoma cell-line;

REFERENCES

[1] M.P. Barrett, R.J. Burchmore, A. Stich, J.O. Lazzari, A.C. Frasch, J.J. Cazzulo, S. Krishna, The trypanosomiases, Lancet. 362 (2003) 1469–1480. doi:10.1016/S0140-6736(03)14694-6.

[2] R. Brun, J. Blum, F. Chappuis, C. Burri, Human African trypanosomiasis, Lancet. 375 (2010) 148–159. doi:10.1016/S0140-6736(09)60829-1.

[3] M.-B. Qian, X.-N. Zhou, Global burden on neglected tropical diseases, Lancet Infect. Dis. 16 (2016) 1113–1114. doi:10.1016/S1473-3099(16)30328-0.

[4] E.K. Elmahallawy, A. Agil, Treatment of leishmaniasis: A review and assessment of recent research, Curr. Pharm. Des. 21 (2015) 2259–2275. doi:10.2174/1381612821666141231163053.

[5] P.G.E. Kennedy, Clinical features, diagnosis, and treatment of human African trypanosomiasis (sleeping sickness), Lancet Neurol. 12 (2013) 186–194. doi:10.1016/S1474-4422(12)70296-X.

[6] J.A. Pérez-Molina, A.M. Perez, F.F. Norman, B. Monge-Maillo, R. López-Vélez, Old and new challenges in Chagas disease, Lancet Infect. Dis. 15 (2015) 1347–1356. doi:10.1016/S1473-3099(15)00243-1.

[7] S. Patterson, S. Wyllie, Nitro drugs for the treatment of trypanosomatid diseases: Past, present, and future prospects, Trends Parasitol. 30 (2014) 289–298. doi:10.1016/j.pt.2014.04.003.

[8] M. Sundar S, Availability of miltefosine for treatment of kala- azar in India., Bull World Heal. Organ. 83 (2005) 394–5.

[9] S.L. Croft, M.P. Barrett, J.A. Urbina, Chemotherapy of trypanosomiases and leishmaniasis, Trends Parasitol. 21 (2005) 508–512. doi:10.1016/j.pt.2005.08.026.

[10] I.H. Gilbert, Drug Discovery for Neglected Diseases: Molecular Target- Based and Phenotypic Approaches, J. Med. Chem. 56 (2013) 7719–7726. doi:10.1021/jm400362b.

[11] DNDi, Phase II Proof of Concept Trial to Determine Efficacy of Fexinidazole in Visceral Leishmaniasis Patients in Sudan, http://clinicaltrials.gov/show/NCT01980199. (n.d.).

[12] S. Gupta, V. Yardley, P. Vishwakarma, R. Shivahare, B. Sharma, D. Launay, D. Martin, S.K. Puri, Nitroimidazo-oxazole compound dndi-vl-2098: An orally effective preclinical drug candidate for the treatment of visceral leishmaniasis, J. Antimicrob. Chemother. 70 (2015) 518–527. doi:10.1093/jac/dku422.

[13] M.P. Costi, CORDIS - Final Report Summary - NMTRYPI (New Medicines for Trypanosomatidic Infections), (n.d.). http://cordis.europa.eu/result/rcn/199861_en.html.

[14] C. Borsari, R. Lucian, C. Pozz, I. Poehner, S. Henrich, M. Trande, A. Cordeiro-Da-silva, N. Santarem, C. Baptista, A. Tait, F. Di Pisa, L. Dello Iacono, G. Landi, S. Gul, M. Wolf, M. Kuzikov, B. Ellinger, J. Reinshagen, G. Witt, P. Gribbon, M. Kohler, O. Keminer, B. Behrens, L. Costantino, P.T. Nevado, E. Bifeld, J. Eick, J. Clos, J. Torrado, M.J. Corral, J. Alunda, F. Pellati, R.C. Wade, S. Ferrari, S. Mangani, M.P. Costi, Profiling of flavonol derivatives for the development of antitrypanosomatidic drugs, J. Med. Chem. 59 (2016) 7598–7616. doi:10.1021/acs.jmedchem.6b00698.

[15] C. Borsari, N. Santarem, J. Torrado, A.I. Olías, M.J. Corral, C. Baptista, S. Gul, M. Wolf, M. Kuzikov, B. Ellinger, J. Reinshagen, P. Linciano, A. Tait, L. Costantino, L.H. Freitas-Junior, C.B. Moraes, P. Bruno dos Santos, L.M. Alcântara, C.H. Franco, C.D. Bertolacini, V. Fontana, P. Tejera Nevado, J. Clos, J.M. Alunda, A. Cordeiro-da-Silva, S. Ferrari, M.P. Costi, Methoxylated 2'-hydroxychalcones as antiparasitic hit compounds, Eur. J. Med. Chem. (2016). doi:10.1016/j.ejmech.2016.12.017.

[16] S. Ferrari, F. Morandi, D. Motiejunas, E. Nerini, S. Henrich, R. Luciani, A. Venturelli, S. Lazzari, S. Calò, S. Gupta, V. Hannaert, P.A.M. Michels, R.C. Wade, M.P. Costi, Virtual screening identification of nonfolate compounds, including a CNS drug, as antiparasitic agents inhibiting pteridine reductase, J. Med. Chem. 54 (2011) 211–221. doi:10.1021/jm1010572.

[17] a R. Bello, B. Nare, D. Freedman, L. Hardy, S.M. Beverley, PTR1: a reductase mediating salvage of oxidized pteridines and methotrexate resistance in the protozoan parasite Leishmania major., Proc. Natl. Acad. Sci. U. S. A. 91 (1994) 11442–11446. doi:10.1073/pnas.91.24.11442.

[18] S.K. Masayuki Uda, Ring-Chain Tautomerism of Aceton N-Methylated Thiosemicarbazones, J. Heterocycl. Chem. 16 (1979) 1273–1275.

[19] K.N. Zelenin, O.B. Kuznetsova, V. V. Alekseyev, P.B. Terentyev, V.N. Torocheshnikov, V. V. Ovcharenko, Ring-Chain Tautomerism of N-Substituted Thiosemicarbazones,

Tetrahedron. 49 (1993) 1257–1270. doi:10.1016/S0040-4020(01)85816-6.

[20] R. Siles, S.-E. Chen, M. Zhou, K.G. Pinney, M.L. Trawick, Design, synthesis, and biochemical evaluation of novel cruzain inhibitors with potential application in the treatment of Chagas' disease., Bioorg. Med. Chem. Lett. 16 (2006) 4405–9. doi:10.1016/j.bmcl.2006.05.041.

[21] D.C. Greenbaum, Z. Mackey, E. Hansell, P. Doyle, J. Gut, C.R. Caffrey, J. Lehrman, P.J. Rosenthal, J.H. McKerrow, K. Chibale, Synthesis and structure-activity relationships of parasiticidal thiosemicarbazone cysteine protease inhibitors against Plasmodium falciparum, Trypanosoma brucei, and Trypanosoma cruzi, J. Med. Chem. 47 (2004) 3212–3219. doi:10.1021/jm030549j.

[22] X. Du, C. Guo, E. Hansell, P.S. Doyle, C.R. Caffrey, T.P. Holler, J.H. McKerrow, F.E. Cohen, Synthesis and structure-activity relationship study of potent trypanocidal thio semicarbazone inhibitors of the trypanosomal cysteine protease cruzain, J. Med. Chem. 45 (2002) 2695–2707. doi:10.1021/jm010459j.

[23] N.C. Fonseca, L.F. Da Cruz, F. Da Silva Villela, G.A. Do Nascimento Pereira, J.L. De Siqueira-Neto, D. Kellar, B.M. Suzuki, D. Ray, T.B. De Souza, R.J. Alves, P.A.S. Júnior, A.J. Romanha, S.M.F. Murta, J.H. McKerrow, C.R. Caffrey, R.B. De Oliveira, R.S. Ferreira, Synthesis of a sugar-based thiosemicarbazone series and structure-activity relationship versus the parasite cysteine proteases rhodesain, cruzain, and Schistosoma mansoni cathepsin B1, Antimicrob. Agents Chemother. 59 (2015) 2666–2677. doi:10.1128/AAC.04601-14.

[24] D.R. Magalhaes Moreira, A.D.T. De Oliveira, P.A. Teixeira De Moraes Gomes, C.A. De Simone, F.S. Villela, R.S. Ferreira, A.C. Da Silva, T.A.R. Dos Santos, M.C.A. Brelaz De Castro, V.R.A. Pereira, A.C.L. Leite, Conformational restriction of aryl thiosemicarbazones produces potent and selective anti-Trypanosoma cruzi compounds which induce apoptotic parasite death, Eur. J. Med. Chem. 75 (2014) 467–478. doi:10.1016/j.ejmech.2014.02.001.

[25] L. Blau, R.F. Menegon, G.H.G. Trossini, J.V.D. Molino, D.G. Vital, R.M.B. Cicarelli, G.D.

Passerini, P.L. Bosquesi, C.M. Chin, Design, synthesis and biological evaluation of new aryl thiosemicarbazone as antichagasic candidates, Eur. J. Med. Chem. 67 (2013) 142–151. doi:10.1016/j.ejmech.2013.04.022.

[26] M. Vieites, L. Otero, D. Santos, J. Toloza, R. Figueroa, E. Norambuena, C. Olea-Azar, G. Aguirre, H. Cerecetto, M. Gonzalez, A. Morello, J.D. Maya, B. Garat, D. Gambino, Platinum(II) metal complexes as potential anti-Trypanosoma cruzi agents., J. Inorg. Biochem. 102 (2008) 1033–1043. doi:10.1016/j.jinorgbio.2007.12.005.

[27] M. Vieites, L. Otero, D. Santos, C. Olea-Azar, E. Norambuena, G. Aguirre, H. Cerecetto, M. Gonzalez, U. Kemmerling, A. Morello, J. Diego Maya, D. Gambino, Platinum-based complexes of bioactive 3-(5-nitrofuryl)acroleine thiosemicarbazones showing anti-Trypanosoma cruzi activity., J. Inorg. Biochem. 103 (2009) 411–418. doi:10.1016/j.jinorgbio.2008.12.004.

[28] L. Otero, M. Vieites, L. Boiani, A. Denicola, C. Rigol, L. Opazo, C. Olea-Azar, J.D. Maya, A. Morello, R.L. Krauth-Siegel, O.E. Piro, E. Castellano, M. González, D. Gambino, H. Cerecetto, Novel Antitrypanosomal Agents Based on Palladium Nitrofurylthiosemicarbazone Complexes: DNA and Redox Metabolism as Potential Therapeutic Targets, J. Med. Chem. 49 (2006) 3322–3331. doi:10.1021/jm0512241.

[29] A. Pérez-Rebolledo, L.R. Teixeira, A.A. Batista, A.S. Mangrich, G. Aguirre, H. Cerecetto, M. González, P. Hernández, A.M. Ferreira, N.L. Speziali, H. Beraldo, 4-Nitroacetophenone-derived thiosemicarbazones and their copper(II) complexes with significant in vitro anti-trypanosomal activity, Eur. J. Med. Chem. 43 (2008) 939–948. doi:https://doi.org/10.1016/j.ejmech.2007.06.020.

[30] G. Pelosi, Thiosemicarbazone Metal Complexes: From Structure to Activity~!2009-12-08~!2010-01-13~!2010-03-25~!, Open Crystallogr. J. 3 (2010) 16–28. doi:10.2174/1874846501003020016.

[31] P. Linciano, A. Dawson, I. Pöhner, D.M. Costa, M.S. S, A. Cordeiro-da-Silva, R. Luciani, S.

Gul, G. Witt, B. Ellinger, M. Kuzikov, P. Gribbon, J. Reinshagen, M. Wolf, B. Behrens, V. Hannaert, P.A.M. Michels, E. Nerini, C. Pozzi, F. di Pisa, G. Landi, N. Santarem, S. Ferrari, P. Saxena, S. Lazzari, G. Cannazza, L.H. Freitas-Junior, C.B. Moraes, B.S. Pascoalino, L.M. Alcantara, C.P. Bertolacini, V. Fontana, U. Wittig, W. Müller, R.C. Wade, W.N. Hunter, S. Mangani, L. Costantino, M.P. Costi, Exploiting the 2-amino-1,3,4-thiadiazole scaffold to inhibit Trypanosoma brucei pteridine reductase in support of early stage drug discovery, ACS Omega. Accepted (2017).

[32] N. Baker, L. Glover, J.C.J.C. Munday, D. Aguinaga Andrés, M.P.M.P. Barrett, H.P.H.P. de Koning, D. Horn, D. Aguinaga Andres, M.P.M.P. Barrett, H.P.H.P. de Koning, D. Horn, Aquaglyceroporin 2 controls susceptibility to melarsoprol and pentamidine in African trypanosomes., Proc. Natl. Acad. Sci. U. S. A. 109 (2012) 10996–1001. doi:10.1073/pnas.1202885109.

[33] C.B. Moraes, M. a Giardini, H. Kim, C.H. Franco, A.M. Araujo-Junior, S. Schenkman, E. Chatelain, L.H. Freitas-Junior, Nitroheterocyclic compounds are more efficacious than CYP51 inhibitors against Trypanosoma cruzi: implications for Chagas disease drug discovery and development., Sci. Rep. 4 (2014) 4703. doi:10.1038/srep04703.

[34] T. Chou, Theoretical Basis, Experimental Design, and Computerized Simulation of Synergism and Antagonism in Drug Combination Studies, Pharmacol. Rev. 58 (2006) 621–681. doi:10.1124/pr.58.3.10.

[35] K. Katsuno, J.N. Burrows, K. Duncan, R.H. van Huijsduijnen, T. Kaneko, K. Kita, C.E. Mowbray, D. Schmatz, P. Warner, B.T. Slingsby, Hit and lead criteria in drug discovery for infectious diseases of the developing world, Nat. Rev. Drug Discov. 14 (2015) 751–8. doi:10.1038/nrd4683.

[36] J. Faria, C.B. Moraes, R. Song, B.S. Pascoalino, N. Lee, J.L. Siqueira-Neto, D.J.M. Cruz, T. Parkinson, J.-R. Ioset, A. Cordeiro-da-Silva, L.H. Freitas-Junior, Drug discovery for human African trypanosomiasis: identification of novel scaffolds by the newly developed HTS

SYBR Green assay for Trypanosoma brucei., J. Biomol. Screen. 20 (2015) 70–81. doi:10.1177/1087057114556236.

[37] T. Bowling, L. Mercer, R. Don, R. Jacobs, B. Nare, Application of a resazurin-based high-throughput screening assay for the identification and progression of new treatments for human african trypanosomiasis, Int. J. Parasitol. Drugs Drug Resist. 2 (2012) 262–270. doi:10.1016/j.ijpddr.2012.02.002.

TOC – Graphical abstract

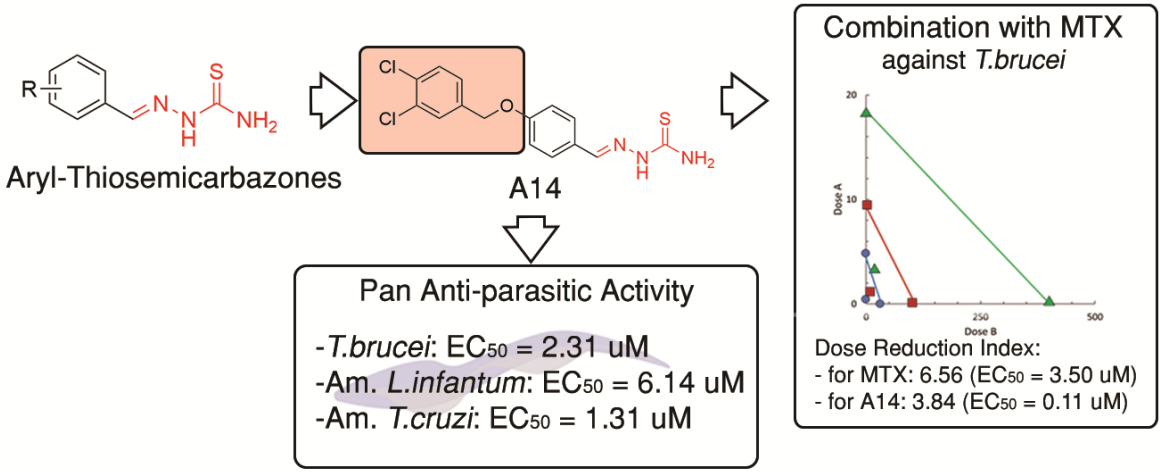

Thiosemicarbazones, thiadiazoles opened form, are compounds of interest for phenotypic screening against *Trypanosoma brucei*, intracellular amastigote form of *Leishmania infantum* and *Trypanosoma cruzi*. Early toxicity profile against human cell lines, *h*ERG, Aurora B, five cytochrome P450 isoforms and mitochondrial toxicity demonstrated the low toxicity for the compounds class in comparison with known drugs. Compound A14, a 3.4-dichlorobenzyl derivative, showed low microMolar EC_{50} against the three parasites and a synergic activity in combination with methotrexate. The results confirmed thiosemicarbazones as a suitable chemical scaffold with potential for the development of new anti-parasitic drugs.